Spin-wave, Stoner single-particle and correlated particle-hole pair contributions to thermal demagnetization in amorphous $Fe_{90+x}Zr_{10-x}$

1991 J. Phys.: Condens. Matter 3 4027

(http://iopscience.iop.org/0953-8984/3/22/013)

J. Phys.: Condens. Matter 3 (1991) 4027–4043. Printed in the UK

Spin-wave, Stoner single-particle and correlated particle–hole pair contributions to thermal demagnetization in amorphous $Fe_{90+x}Zr_{10-x}$ alloys

S N Kaul
School of Physics, University of Hyderabad, Central University PO, Hyderabad 500134, India

Received 4 May 1990, in final form 26 November 1990

Abstract. Detailed magnetization (M) measurements have been performed on amorphous (a-)$Fe_{90+x}Zr_{10-x}$ alloys with $x = 0$ and 1 at temperatures ranging from 4.2 to 300 K in external magnetic fields (H) up to 15 kOe. Arrott plot isotherms of $M^2(H, T)$ against $H/M(H, T)$ are nearly linear at high magnetic fields for temperatures well outside the critical region. Spontaneous magnetization varies with temperature as $M(0, T)/M(0, 0) = 1 - BT^{3/2} - AT^2$, $[M(0, T)/M(0, 0)]^2 = a - bT^2$ and $[M(0, T)/M(0, 0)]^2 = a' - b'T^{4/3}$ in the temperature intervals $0 \lesssim T \lesssim 0.38T_C$ (Curie temperature), $0.39T_C \lesssim T \lesssim 0.9T_C$ and $0.91T_C \lesssim T \lesssim 0.98T_C$, respectively. These results can be adequately described by the theory that includes corrections to the conventional Stoner model arising from enhanced fluctuations in the local spin density. An elaborate analysis of highly accurate 'in-field' magnetization data for the first time permits an unambiguous separation of spin-wave (Δm_{sw}) and single-particle (Δm_{sp}) contributions to the thermal demagnetization (Δm) and reveals that: (i) contrary to the previous finding, the spin-wave stiffness coefficient D is *independent* of H; (ii) the spin-density fluctuations get *strongly suppressed* by the external field; (iii) spin-wave modes *soften* at low temperatures where the ferromagnetic state gives way to a 'mixed magnetic state'; (iv) the D/T_C ratio possesses a value of about 0.14 *typical* of amorphous ferromagnets with competing interactions while Δm_{sp} has a sizable value *characteristic* of Invar systems; and (v) the competing interactions confine the direct Heisenberg exchange interaction to the nearest neighbours only. A straightforward explanation has been provided for the absence of spin-wave peaks in the inelastic neutron scattering spectra taken on a-$Fe_{91}Zr_9$ in the wavevector transfer range of $0.05\ \text{Å}^{-1} \lesssim q \lesssim 0.12\ \text{Å}^{-1}$ in terms of a model previously proposed by the author in connection with the static critical phenomena in amorphous alloys including those investigated in this work.

1. Introduction

Amorphous (a-)$Fe_{90+x}Zr_{10-x}$ ($0 \lesssim x \lesssim 3$) alloys have attracted considerable scientific attention ever since a rich variety of novel physical phenomena, e.g. weak itinerant-electron ferromagnetism (Kaul 1983a), Invar effect (Shirakawa *et al* 1980), re-entrant spin-glass (RSG) behaviour at low temperatures (Hiroyoshi and Fukamichi 1982, Kaul 1983a), broad distribution of magnetic hyperfine fields with finite probability even at zero field (Kaul *et al* 1988, Siruguri *et al* 1988, 1990) and electrical resistivity minima (Obi *et al* 1982, Kaul *et al* 1990) at temperatures close to the Curie temperature T_C, were discovered in them. An in-depth study of their magnetic properties, in particular, has

0953-8984/91/224027 + 17 $03.50

lately assumed greater importance owing to the claim that the long-range ferromagnetic ordering does not develop in these alloys at any temperature made by Rhyne and Fish (1985) on the basis of small-angle neutron scattering (SANS) data taken on a-$Fe_{91}Zr_9$ alloy in the wavevector transfer range of $0.04\ \text{Å}^{-1} \leq q \leq 0.20\ \text{Å}^{-1}$, which indicate that the correlation length for the critical spin fluctuations, ξ, does not diverge at T_C but remains finite ($\lesssim 30$ Å) from T_C down to 4.2 K. This SANS result has also led some workers to propose physical descriptions of the magnetic order for $T < T_C$ such as a 'wandering-axis ferromagnet', in which the spin structure is *locally ferromagnetic* (Ryan *et al* 1987) with small variations in spin directions on neighbouring sites but the local ferromagnetic axis changes direction over distances of order ξ, or a strongly exchange-frustrated system in which the *ferromagnetic corrections* are *short-ranged* $\leq \xi$ (Fish and Rhyne 1987). Subsequently, based on Mössbauer (Kaul *et al* 1988, Siruguri *et al* 1988, 1990), bulk magnetization (Kaul 1988), AC susceptibility (Kaul *et al* 1986, Kaul 1987, 1988) and ferromagnetic resonance (Kaul and Siruguri 1991, Kaul and Veera Mohan 1991) data on the alloys with $x = 0$, 1 and 2, we have demonstrated that: (i) a second-order phase transition, characterized by three-dimensional (3D) Heisenberg-like critical exponent values, from the paramagnetic state ($T > T_C$) to a state with *long-range ferromagnetic order* ($T < T_C$) occurs at T_C ($T_C = 240 \pm 1$ K and 210 ± 1 K for a-$Fe_{90}Zr_{10}$ and a-$Fe_{91}Zr_9$ alloys, respectively); (ii) none of the above-mentioned physical pictures (Ryan *et al* 1987, Fish and Rhyne 1987), but a model (Kaul 1984a, 1985) that considers the spin system for $T < T_C$ to consist of *finite spin clusters* embedded in, but 'isolated' from, an *infinite 3D ferromagnetic matrix*, forms an adequate description of the type of magnetic order present in such glassy materials; and (iii) the apparent contradiction between the bulk magnetization and SANS results stems from the fact that the SANS response in the q range $0.04\ \text{Å}^{-1} \leq q \leq 0.20\ \text{Å}^{-1}$ is completely dominated by the finite spin clusters and the fact that SANS measurements need to be extended to sufficiently low q values ($q \ll 0.04\ \text{Å}^{-1}$) to observe the expected divergence in $\xi(T)$ at $T = T_C$. Recent high-resolution SANS studies (Rhyne *et al* 1988) on a-$Fe_{100-x}Zr_x$ alloys with $x = 8$, 9 and 10 in the q range $0.008\ \text{Å}^{-1} \leq q \leq 0.02\ \text{Å}^{-1}$ lend firm support to our assertions (ii) and (iii) above.

In a continued effort to unravel the exact nature of magnetism in the amorphous alloys in question, we address ourselves to yet another controversial aspect of ferromagnetism in a-$Fe_{90\pm x}Zr_{10\mp x}$ alloys, i.e. the existence of spin-wave excitations, in this paper. Early bulk magnetization measurements (Kaul 1983a) on a-$Fe_{90}Zr_{10}$ alloy revealed that the temperature dependence of magnetization in fixed magnetic fields, $M(H, T)$, up to 15 kOe for $T \leq 0.5T_C$, is better described by a T^2 power law, representing the Stoner single-particle contribution, than by a $T^{3/2}$ law, denoting the spin-wave contribution, but both the power laws provide equally good fits to $M(H, T)$ data for $T \gtrsim 0.5T_C$. For the alloy with the same nominal composition, Krishnan *et al* (1984) later found that $M(H, T) \propto T^{3/2}$ for $T > T^*$ in external magnetic fields up to 140 kOe (T^* shifts to *higher* temperatures for *lower* field values) and attributed the deviations from the $T^{3/2}$ power law for $T < T^*$ to the breakdown of long-range ferromagnetic order and the onset of spin-glass behaviour even though T^* ($\simeq 0.5T_C \simeq 120$ K) is about three times greater than the RSG transition temperature, T_{RSG} ($= 40 \pm 1$ K; Kaul 1983a). They also noticed that the spin-wave stiffness coefficient D *increases* with *increasing* H and attains a value of 39.1 meV Å^2 at $H = 140$ kOe. Contrasted with these findings, Beck and Kronmüller (1985) observed that the variation of magnetization with temperature in the temperature range $5\ \text{K} \leq T \leq 0.5T_C$ for a-$Fe_{90.6}Zr_{9.4}$ alloy is best described by the expressions $M(H, T) = M(H, 0) - C_2(H)T^2$ for $H < 2.7$ kOe and $M(H, T) = M(H, 0) - C_{3/2}(H)T^{3/2} - C_{5/2}(H)T^{5/2}$ for $H \geq 2.7$ kOe and that D *decreases* from 50 to

35 meV Å^2 as H is *increased* from 2.7 to 40 kOe. The situation is further complicated by the outcome of the inelastic neutron scattering studies (Fish and Rhyne 1987) on a-$Fe_{91}Zr_9$ alloy that no propagating excitations can be detected at any temperature $T < T_C$ for $0.05\ Å^{-1} \leqslant q \leqslant 0.12\ Å^{-1}$ even with an energy resolution limit as high as $E = 120\ \mu eV$ and that the linewidth and resolution analysis places an upper bound on the value of D of 12–15 meV Å^2. A close scrutiny of the existing bulk magnetization data reveals that both single-particle and spin-wave excitations contribute to the thermal demagnetization in these alloys and their contributions are comparable in magnitude. Under these circumstances, the actual value of the spin-wave stiffness coefficient can be extracted (Kaul 1984b) from magnetization data only when an *unambiguous* separation of the single-particle and spin-wave contributions is made possible by an accuracy in magnetization measurements far exceeding that accomplished so far in the literature.

2. Experimental details

Amorphous $Fe_{90}Zr_{10}$ and $Fe_{91}Zr_9$ alloys were prepared in the form of ribbons (2–3 mm in width and 30–40 μm in thickness) under a helium atmosphere by a single-roller melt quenching technique. The amorphous nature of the fabricated alloys was confirmed by high-resolution electron microscopy. Using the Faraday method, highly accurate (relative accuracy better than 10 ppm) magnetization measurements were performed on the same samples of amorphous (a-)$Fe_{90+x}Zr_{10-x}$ alloys ($x = 0$ and 1) as used previously for static critical phenomena studies (Kaul *et al* 1986, Kaul 1988). The present investigation involves the measurement of magnetization M as a function of temperature in the temperature range 4.2 to 300 K at several fixed values of the external magnetic field H in the interval 5 kOe $\leqslant H \leqslant$ 15 kOe (upper instrumental limit) during the *cooling cycle* and M versus H isotherms at different temperatures in the above-mentioned temperature range in fields up to 15 kOe. Reasons for using fields $H \geqslant 5$ kOe for $M(T)$ measurements are twofold. First, the irreversible effects associated with the 'spin-glass-like' behaviour at low temperatures are suppressed to a large extent at such field strengths. Secondly, high resolution of $\leqslant$10 ppm in magnetization measurements could be achieved only for fields $H \gtrsim 4$ kOe because the field gradient that the sample experiences increases with the 'base-field'.

3. Results, analysis and discussion

Now that both the glassy alloys in question are found to exhibit nearly the same magnetic behaviour, it suffices to describe in detail the results and analysis for a-$Fe_{90}Zr_{10}$ only and to quote the final values for important parameters in the case of a-$Fe_{91}Zr_9$.

3.1. Magnetic equation of state and spontaneous magnetization

Previous bulk magnetization measurements (Kaul 1983a) carried out on the a-$Fe_{90}Zr_{10}$ sample taken from a batch different from the present one revealed that: (i) magnetization $M(H, T)$ does not saturate in fields up to 15 kOe at low temperatures; the high-field susceptibility at the lowest temperature 4.2 K has a value $(15.0 \pm 0.5) \times 10^{-5}$ emu g^{-1} Oe^{-1}; (ii) the Arrott plot isotherms of the form $M^2(H, T)$ versus $H/M(H, T)$

are *linear* over a wide range in the magnetic field H and temperature T at high fields (with considerable departure from linearity at low fields); and (iii) the spontaneous magnetization decreases with temperature as

$$[M(0, T)/M(0, 0)]^2 = 1 - 2AT^2 \tag{1}$$

for $T \leqslant 0.375T_C$ with $A = (11.44 \pm 0.16) \times 10^{-6}\,K^{-2}$. The properties (ii) and (iii) can be *qualitatively* understood in terms of the theory, based on the Stoner model in which a temperature-independent one-particle density of states is Zeeman split into the spin-up and spin-down components by an exchange (molecular) field λM characterized by a temperature-independent interaction constant λ, proposed for very weak itinerant ferromagnets by Edwards and Wohlfarth (1968) as follows. For very weak itinerant ferromagnets (small M limit), at all temperatures from 0 K to just below T_C and from just above T_C to higher temperatures so long as $T \ll T_F$, this theory yields a magnetic equation of state of the form

$$H = a(T)M(H, T) + bM^3(H, T) \tag{2}$$

with

$$a(T) = -(\tfrac{1}{2})\chi^{-1}(0, 0)\,[1 - (T/T_C)^2] \tag{3}$$

$$b = (\tfrac{1}{2})\chi^{-1}(0, 0)\,[M(0, 0)]^{-2} \tag{4}$$

and zero-field differential susceptibility at 0 K, $\chi(0, 0)$, given by

$$\chi(0, 0) = N\mu_B^2 N(E_F)\,(T_F/T_C)^2 \tag{5}$$

where

$$T_F^{-2} = (\pi^2 k_B^2/6)\,\{[N'(E_F)/N(E_F)]^2 - [N''(E_F)/N(E_F)]\}. \tag{6}$$

Here N is the number of atoms per unit volume, $N(E_F)$ is the density of single-particle states at the Fermi level E_F and $N'(E_F)$ $[N''(E_F)]$ is its first (second) energy derivative. While property (ii) is an immediate consequence of the form of equation (2) and the weak field dependence of the coefficients a and b, property (iii) derives its origin from equations (2)–(4) as is evident from the following calculation. Equation (2) gives the spontaneous magnetization $M(0, T)$ as $M^2(0, T) = -a(T)/b$. After substituting for $a(T)$ and b from equations (3) and (4) and rearranging the terms, one obtains

$$[M(0, T)/M(0, 0)]^2 = 1 - (T/T_C)^2. \tag{7}$$

A comparison of equation (7) with equation (1) demonstrates that

$$A = \tfrac{1}{2}T_C^{-2}. \tag{8}$$

The experimentally determined (Kaul 1983a) value of $T_C = 240$ K when used in equation (8) yields an estimate for $A = 8.68 \times 10^{-6}\,K^{-2}$, which is about three-quarters of the observed value. The above model invariably overestimates T_C, and the predicted coefficient of the Stoner T^2 term is, therefore, more than one order of magnitude smaller than that actually observed. Following the realization that the *failure* of the Stoner theory to predict the Curie temperature correctly and to provide an explanation for the Curie–Weiss behaviour of the magnetic susceptibility, generally observed in a wide variety of magnetic materials for temperatures above T_C, is primarily due to its underlying assumption that the thermally excited electrons and holes move *independently* in a common mean field, numerous attempts (for comprehensive reviews, see Moriya

(1979, 1983) and references cited therein) have been made in the last two decades to take into account the collective nature of the electron–hole excitations. The most noteworthy among these theoretical attempts is the *quantitative* model for nearly ferromagnetic metals or ferromagnetic metals with *unsaturated* moments due to Lonzarich and Taillefer (1985), which goes beyond the earlier theoretical treatments in including the *transverse* as well as the *longitudinal* local spin-density fluctuations, in incorporating a natural temperature-dependent cut-off wavevector for the thermally excited modes and in using band-structure and other parameters appropriate to known weakly magnetic metals like Ni_3Al and MnSi rather than to the special electron-gas model (Moriya and Kawabata 1973), and obtains a good *quantitative* agreement with the experiment for the magnitude of T_C, the ratio p_{eff}/p_0 of the high- to low-temperature effective moments and the coefficient of the quadratic (T^2) variation of spontaneous magnetization with temperature well below T_C. This model (Lonzarich and Taillefer 1985) predicts *nearly linear* $M^2(H, T)$ versus $H/M(H, T)$ isotherms at high magnetic fields (i.e. a magnetic equation of state of the form given by equation (2) is valid at large field strengths only) in ferromagnetic as well as paramagnetic regimes and the temperature dependence of the spontaneous magnetization of the type

$$[M(0, T)/M(0, 0)] = 1 - BT^{3/2} \tag{9}$$

at very low temperatures,

$$[M(0, T)/M(0, 0) \simeq [1 - (T/T_C)^2]^{1/2} \tag{10}$$

over a wide range of intermediate temperatures and

$$[M(0, T)/M(0, 0)] = [1 - (T/T_C)^{4/3}]^{1/2} \tag{11}$$

for temperatures close to T_C. This model is, however, not expected to yield the exact behaviour of spontaneous magnetization in the critical region even though it correctly predicts a second-order magnetic phase transition at T_C because it completely neglects the critical fluctuations of the order parameter.

That this theory is applicable to the non-crystalline ferromagnetic systems under consideration as well is indicated by the observations that the magnetization does not saturate even in fields as high as 190 kOe (Hiroyoshi *et al* 1983, Krishnan *et al* 1984, Ryan *et al* 1987) at low temperatures in these materials and the Arrott plot isotherms are *approximately linear* only for very high values of the external magnetic field over a wide range of temperatures (Hiroyoshi *et al* 1983). Figure 1 shows $M^2(H, T)$ plotted against $H/M(H, T)$ in the critical region for a-$Fe_{90}Zr_{10}$, while the M^2 versus H/M isotherms taken at the end temperatures 4.2 and 296 K of the temperature range covered in the present experiments are shown in the insets. In accordance with the theoretical (Lonzarich and Taillefer 1985) predictions, M^2 versus H/M isotherms are *roughly linear* at high fields for temperatures well outside the critical region (insets of figure 1, and figures 4 and 5 in the papers by Kaul (1983a) and Hiroyoshi *et al* (1983), respectively). By contrast, the Arrott plot isotherms present a slight but finite curvature even at fields $H \gtrsim 15$ kOe (see figure 1, and also figure 5 in the paper by Hiroyoshi *et al* (1983)) in the critical region (note that this observation brings out the main limitation of the theory proposed by Lonzarich and Taillefer (1985) in that the mean-field approximation, on which this theory is based, is bound to yield erroneous results in this temperature range). Curvature in the high-field portion of the M^2 versus H/M isotherms makes an accurate determination of spontaneous magnetization impossible because an extrapolation of these high-field portions to zero field cannot be carried out unambiguously. To tackle

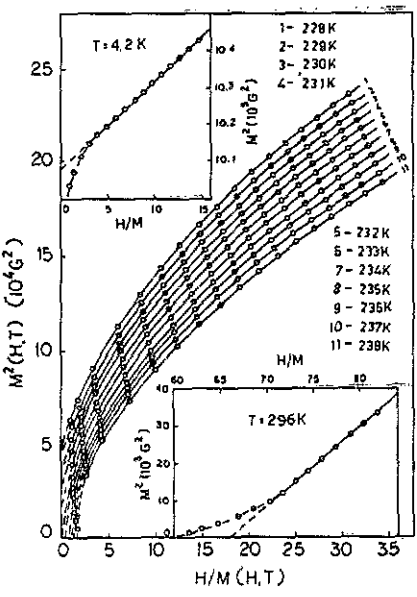

Figure 1. Arrott plot (M^2 versus H/M) isotherms for a-$Fe_{90}Zr_{10}$ in the critical region. Insets show such isotherms for the end temperatures of the investigated temperature range.

this problem effectively, the isotherms are made exactly linear over a wide range of fields especially in the high-field region by allowing the critical exponents β and γ for the spontaneous magnetization and initial susceptibility in the modified Arrott plots of $M^{1/\beta}$ against $(H/M)^{1/\gamma}$ to vary with temperature such that they assume three-dimensional Heisenberg-like values ($\beta \simeq 0.36$, $\gamma \simeq 1.38$) in the critical region (Kaul 1988) and mean-field values ($\beta = 0.5$, $\gamma = 1.0$) for temperatures far away from T_C ($T \lesssim T_C$) and then these high-field straight-line portions are linearly extrapolated to $(H/M) = 0$ in order to arrive at accurate values of spontaneous magnetization $M(0, T)$ for $T \lesssim T_C$. The $M(0, T)$ data so obtained are plotted in the form $[M(0, T)/M(0, 0)]^2$ versus T^2 and $[M(0, T)/M(0, 0)]^2$ versus $T^{4/3}$ in figure 2 with a view to ascertaining the exact functional dependence of spontaneous magnetization on temperature. It is evident from these plots that, out of the two power laws, the T^2 law describes the variation of $[M(0, T)/M(0, 0)]^2$ with temperature better in the temperature ranges $0 \lesssim T \lesssim 0.39T_C$ and $0.4T_C \lesssim T \lesssim 0.9T_C$, whereas both the power laws seem to fit the $[M(0, T)/M(0, 0)]^2$ data equally well in the range $0.9T_C \lesssim T \lesssim 0.98T_C$. A detailed analysis, however, reveals that

$$\frac{\Delta M(0,T)}{M(0,0)} = \frac{M(0,0) - M(0,T)}{M(0,0)} = \frac{g\mu_B}{M(0,0)}\left(\frac{k_B T}{4\pi D_0(1 - D_2T^2)}\right)^{3/2} + AT^2 \qquad (12)$$

for $0 \leqslant T \leqslant 0.38T_C$ with $g = 2.07 \pm 0.02$ (Kaul and Siruguri 1991), $M(0, 0) = 1\,\mathrm{kG}$, $D_0 = 24 \pm 1\,\mathrm{meV\,\AA^2}$, $D_2 = (1.6 \pm 0.2) \times 10^{-6}\,\mathrm{K^{-2}}$ and $A = (1.5 \pm 0.3) \times 10^{-6}\,\mathrm{K^{-2}}$ (these parameter values when used in equation (12) yield the best least-squares fit, denoted by the full curve in inset (*a*) of figure 2, to the $\Delta M(0, T)/M(0, 0)$ data),

$$[M(0, T)/M(0, 0)]^2 = (0.970 \pm 0.001) - (1.880 \pm 0.005) \times 10^{-5}T^2 \qquad (13)$$

for $0.39T_C \leqslant T \leqslant 0.90T_C$ and

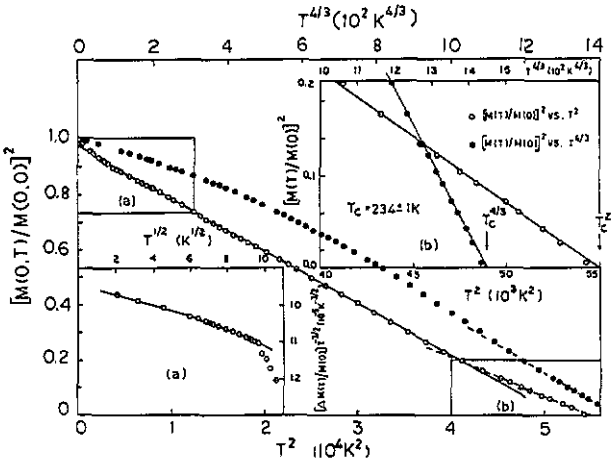

Figure 2. Normalized spontaneous magnetization plotted against temperature in the form $[M(0, T)/M(0, 0)]^2$ versus T^2 and $[(M(0, T)/M(0, 0)]^2$ versus $T^{4/3}$ for amorphous $Fe_{90}Zr_{10}$. In the inset (*a*), $[\Delta M(0, T)/M(0, 0)]/T^{3/2}$ is plotted against $T^{1/2}$; whereas in the inset (*b*), $[M(0, T)/M(0, 0)]^2$ is plotted against T^2 and $T^{4/3}$ in the temperature range $0.91T_C$ to $0.98T_C$.

$$[M(0, T)/M(0, 0)]^2 = (1.097 \pm 0.001) - (7.572 \pm 0.001) \times 10^{-4}T^{4/3} \tag{14}$$

provide a decidedly better least-squares fit, as inferred from a much lower value (by about 1.5 times) for the sum of deviation squares, than

$$[M(0, T)/M(0, 0)]^2 = (0.76 \pm 0.01) - (1.38 \pm 0.03) \times 10^{-5}T^2 \tag{15}$$

in the temperature range $0.91T_C \leqslant T \leqslant 0.98T_C$. The least-squares fits (13)–(15) are represented by the straight lines drawn through the data points in figure 2 and its inset (*b*). The first and second terms in equation (12) denote the spin-wave and single-particle contributions, whose details are given in the following subsection, to thermal demagnetization, respectively. The value for T_C deduced from the least-squares fit based on the $T^{4/3}$ (T^2) power law, i.e. equation (14) (equation (15)), $T_C = 234.9 \pm 0.1$ K ($T_C = 234.6 \pm 0.2$ K) is fairly close to that ($T_C = 233.00 \pm 0.05$ K) determined by the asymptotic analysis of the magnetization data in the critical region (Kaul 1988) where spontaneous magnetization follows the power law $M(0, T) \sim [1 - (T/T_C)]^\beta$ with the value for the critical exponent β given as $\beta = 0.36 \pm 0.02$. A comparison between the relations (12)–(14) and (9)–(11) asserts that both spin-wave and Stoner single-particle excitations make a significant contribution to the decline of spontaneous magnetization with increasing temperature for $T \leqslant 0.38T_C$ whereas the enhanced spin-density fluctuations are primarily responsible for the thermal demagnetization of the spontaneous magnetization for $T > 0.38T_C$.

3.2. 'In-field' magnetization

Figure 3 shows the reduced magnetization squared, i.e. $[M(H, T)/M(H, 0)]^2$, plotted against T^2 and $T^{4/3}$ at $H = 9$ kOe for a-$Fe_{90}Zr_{10}$. The overall features of these curves are also representative of those observed for this alloy as well as for a-$Fe_{91}Zr_9$ at different fixed values of the external magnetic field ranging from 5 to 15 kOe. From these plots,

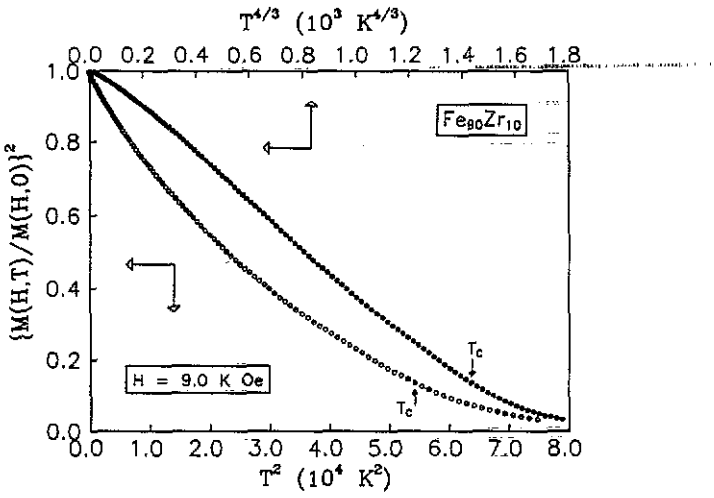

Figure 3. Plots of the reduced 'in-field' magnetization squared, i.e. $[M(H, T)/M(H, 0)]^2$, against T^2 and $T^{4/3}$ for amorphous $Fe_{90}Zr_{10}$.

it is evident that none of these power laws holds for any range of temperatures either well below or close to T_C. An obvious inference from this result is that the spin-density fluctuations get strongly suppressed in the presence of an external magnetic field. Instead of attempting a quantitative comparison of the $M(H, T)$ data with the predictions of theory (Takeuchi and Masuda 1979), which takes into account the effect of an external magnetic field on spin-density fluctuations, a different approach is adopted in which the prime concern is to find out whether or not the observed temperature dependence of the 'in-field' magnetization can be completely accounted for in terms of the spin-wave and/or single-particle excitations. The above preference is justified on the grounds that the theory of Takeuchi and Masuda (1979) totally neglects the spin-wave excitations (which turn out to be of utmost importance in the present case), involves two inter-dependent but unknown parameters and is based on an unrealistic assumption of the electron-gas model. Thus, the functional dependence of the relative deviation of magnetization from its value at 0 K (no distinction between the values of M at 4.2 and 0 K is made in this work), i.e. $[M(H, 0) - M(H, T)]/M(H, 0) \equiv \Delta m$, on temperature is analysed in terms of the expression

$$\Delta m = \Delta m_{sw} + \Delta m_{sp} \tag{16}$$

where the spin-wave, Δm_{sw}, and single-particle, Δm_{sp}, contributions to Δm are given by (Keffer 1966, Mathon and Wohlfarth 1968)

$$\Delta m_{sw} = \frac{g\mu_B}{M(H,0)}\left[Z(\tfrac{3}{2}, t_H)\left(\frac{k_B T}{4\pi D(T)}\right)^{3/2} + 15\pi\beta Z(\tfrac{5}{2}, t_H)\left(\frac{k_B T}{4\pi D(T)}\right)^{5/2}\right] \tag{17}$$

$$\Delta m_{sp} = S(H)T^{\alpha}\exp(-\Delta/k_B T). \tag{18}$$

In equation (17), the Bose–Einstein integral functions

$$Z(s, t_H) = \xi(s)F(s, t_H) = \sum_{n=1}^{\infty} n^{-s} \exp(-nt_H) \tag{19}$$

with

$$t_H = T_g/T = g\mu_B H_{eff}/k_B T \tag{20}$$

allow for the extra energy gap, $g\mu_B H_{eff}$ ($=k_B T_g$), in the spin-wave spectrum arising from the effective field

$$H_{eff} = H - 4\pi NM(0, 0) + H_A \tag{21}$$

where N is the demagnetizing factor, $M(0, 0)$ is the spontaneous magnetization and H_A is the anisotropy field, which the spins experience within the sample. Alternatively, in the presence of the external magnetic field H, the magnon dispersion relation takes the form

$$E_q(T) = \hbar\omega_q(T) = g\mu_B H_{eff} + D(T)q^2(1 - \beta q^2) \tag{22}$$

with the mean-square range of exchange interaction $\langle r^2 \rangle = 20\beta$. For both localized- (Keffer 1966) and itinerant-electron (Izuyama and Kubo 1964, Mathon and Wohlfarth 1968) models, spin-wave energy renormalizes according to the relation

$$D(T) = D_0(1 - D_2 T^2 - D_{5/2} T^{5/2}). \tag{23}$$

Within the framework of the Heisenberg model, the T^2 term appears in the expression for $D(T)$ if the localized d spins interact with one another via conduction s electrons, whereas the $T^{5/2}$ term arises from the magnon–magnon interactions; the T^2 term is, however, several orders of magnitude smaller than the $T^{5/2}$ term since the s–d interaction is very weak compared to the direct d–d interaction. By contrast, the T^2 term, in the itinerant-electron model, results from the interaction between spin waves and single-particle excitations and dominates over the $T^{5/2}$ term, which originates from the magnon–magnon interactions as in the localized-electron case. The following expressions

$$D(T) = D_0(1 - D_2 T^2) \tag{24}$$

and

$$D(T) = D_0(1 - D_{5/2} T^{5/2}) \tag{25}$$

are, therefore, used in this paper to denote the variation of the spin-wave stiffness coefficient with temperature for the itinerant- and localized-electron models, respectively. Furthermore, equation (18) gives a general expression for Δm_{sp} which reduces to more familiar expressions (Mathon and Wohlfarth 1968)

$$\Delta m_{sp} = S(H)T^2 \qquad \text{when } \alpha = 2, \Delta = 0 \tag{26}$$

and

$$\Delta m_{sp} = S(H)T^{3/2} \exp(-\Delta/k_B T) \qquad \text{when } \alpha = 3/2, \Delta \neq 0 \tag{27}$$

for *weak* and *strong* itinerant ferromagnets, respectively.

Having determined the demagnetizing factor N from the low-field magnetization measurements and the splitting factor g ($=2.07 \pm 0.02$) and anisotropy field H_A, from ferromagnetic resonance measurements (Kaul and Siruguri 1991), theoretical fits to the Δm data have been attempted based on equations (16)–(21) with $D(T)$ in equation (17) given by either equation (24) or (25). When the least-squares fit involving seven

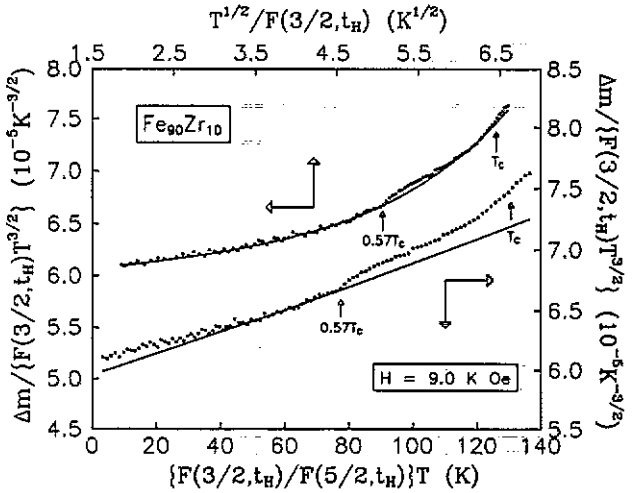

Figure 4. Plots of $\Delta m(9\text{ kOe}, T)/F(\frac{3}{2}, t_H)T^{3/2}$ against $T^{1/2}/F(\frac{3}{2}, t_H)$ and $[F(\frac{3}{2}, t_H)/F(\frac{5}{2}, t_H)]T$ for amorphous $Fe_{90}Zr_{10}$. The full curves through the data points are the best least-squares fits to the data based on the expressions that combine equations (16), (17), (24) and (26) with either $\beta = 0$ or $S = 0$.

parameters, i.e. $M(H, 0)$, D_0, D_2 $(D_{5/2})$, β, S, α and Δ yielded the result $\alpha = 2.00 \pm 0.05$ and $\Delta/k_B = 0 \pm 1$ K, α and Δ were set equal to 2 and 0, respectively, in the subsequent fits, which either use equation (16) with Δm_{sw} and Δm_{sp} represented by equations (17) and (26) or exclude the higher-order spin-wave term, i.e. the $T^{5/2}$ term, or the single-particle contribution (the T^2 term) or both. Such fits in the temperature range $0 \lesssim T \lesssim 0.6T_C$ reveal that a combination of the $T^{3/2}$ and T^2 terms in equation (16) with $D(T) = D_0(1 - D_2T^2)$ reproduces the observed variation of Δm with T most closely as inferred from the lowest value of the sum of deviation squares (χ^2). The plots of $\Delta m(9\text{ kOe}, T)/F(\frac{3}{2}, t_H)T^{3/2} \equiv \Delta m'$ versus $T^{1/2}/F(\frac{3}{2}, t_H)$ and $\Delta m'$ versus $[F(\frac{5}{2}, t_H)/F(\frac{3}{2}, t_H)]T$ for a-$Fe_{90}Zr_{10}$ shown in figure 4 clearly demonstrate that a combination of $T^{3/2}$ and T^2 terms in equation (16) with $D(T)$ in equation (17) given by (24) gives a decidedly better (roughly 1.5 times lower χ^2) fit to the observed $\Delta m(H, T)$ than a combination of $T^{3/2}$ and $T^{5/2}$ terms, i.e. only the spin-wave term in equation (16) with $D(T) = D_0(1 - D_2T^2)$, particularly for temperatures up to $\simeq 0.6T_C$; in the temperature range $0.3T_C \lesssim T \lesssim 0.6T_C$, however, both these combinations seem to fit the data equally well. Note that the strong departure of the data from the latter fit for $T \lesssim 0.3T_C$ could be an artifact of a conventional least-squares (LS) fit method which implicitly gives more weight to the high-temperature data than to the low-temperature data because the *larger magnitude* of the quantity $\Delta m'$ at high temperatures proves to be *decisive* in reducing χ^2. This deficiency of this fitting method could be remedied by employing the *weighted* least-squares method, which counteracts this tendency by giving more weight to the data at low temperatures than to those at high temperatures. We do not, however, pursue this approach simply because Δm data do not exhibit any such deviations when they are fitted to the expression that combines equations (16), (17), (24) and (26), and in which β is set equal to zero, by using the conventional LS method. In order to ascertain the relative importance of the spin-wave and single-particle contributions to Δm at higher temperatures, a 'range-of-fit' analysis has been carried out in which the values of *free*

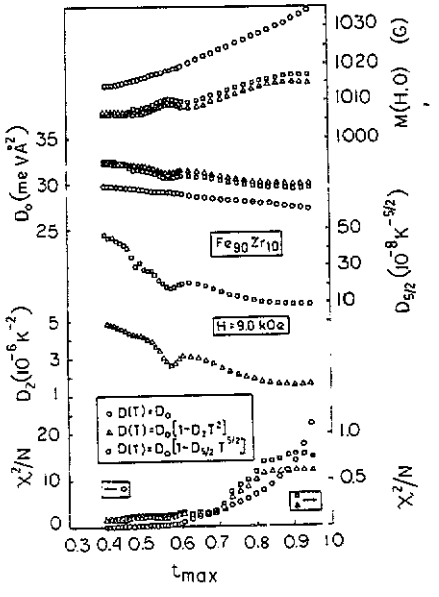

Figure 5. Variation of the free fitting parameters with the upper limit (t_{max}) of the temperature range $t_{min} \leqslant t = (T/T_C) \leqslant t_{max}$ when t_{min} is fixed at 0.3 and the least-squares fits to the in-field magnetization data taken at $H = 9$ kOe are attempted based on equations (16) and (17) with $\beta = \Delta m_{sp} = 0$ and $D(T)$ in equation (17) given by either $D(T) = D_0$, open circles, or equation (24), open triangles, or equation (25), open squares.

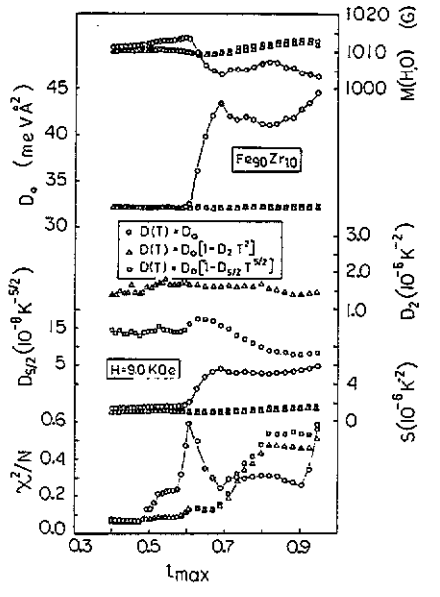

Figure 6. Variation of the free fitting parameters with the upper limit (t_{max}) of the temperature range $t_{min} \leqslant t = (T/T_C) \leqslant t_{max}$ when t_{min} is fixed at 0.3 and the least-squares fits to the $M(H = 9$ kOe, $T)$ data are attempted based on equations (16), (17) and (26) with $\beta = 0$ and $D(T)$ in equation (17) given by either $D(T) = D_0$, open circles, or equation (24), open triangles, or equation (25), open squares.

fitting parameters in 12 different LS fits, based on equations (16), (17) and (26) *rewritten* in the form $M(H, T) = M(H, 0)(1 - \Delta m)$ and involving the combinations $D(T) = D_0$ or $D(T) = D_0(1 - D_2T^2)$ or $D(T) = D_0(1 - D_{5/2}T^{5/2})$ with either $\beta = S = 0$ or $\beta = 0$, $S \neq 0$ or $\beta \neq 0$, $S = 0$ or $\beta \neq 0$, $S \neq 0$, are monitored as the temperature interval $t_{min} \leqslant t = (T/T_C) \leqslant t_{max}$ is progressively broadened by keeping t_{min} fixed at 0.3 and varying t_{max} from 0.4 to 0.95. The results of this analysis with the exception of the case in which $\beta \neq 0$, $S \neq 0$ are depicted in figures 5–7. In these plots, we define a *reduced* χ^2 as χ^2 for the $M(H, T)$ data in a given temperature interval divided by the total number of data points in that interval so as to make a comparison between the parameter values obtained in different temperature intervals physically meaningful and to be able to judge the quality of such fits as a function of t_{max}. (Note that a definition $\chi^2/(N - N_{para})$, where N_{para} is the number of free fitting parameters, would have been a better choice, but this definition of reduced χ^2 gives rise to severe problems when N is not very large as compared to N_{para}; in the present work, such a situation arises for $t_{max} \simeq 0.4$, when the value of $\chi^2/(N - N_{para})$ becomes sensitive to the choice of N_{para} so that it is difficult to decide between different LS fits, but when $t_{max} \gtrsim 0.45$, $N \gg N_{para}$ and no such effect is observed.) Judging by the value of the reduced χ^2 and by the stability of the fitting parameters against a wide variation in t_{max}, the following observations can be made from the data presented in

figures 5–7. (i) Out of all the fits attempted, the one based on the theoretical expression that combines equations (16), (17), (24) and (26) and sets $\beta = 0$ forms the best description of the observed variation of Δm with T for $T \leq 0.7T_C$ whereas for $T > 0.7T_C$ the spin-wave contribution Δm_{sw} (equation (17) with $D(T)$ given by (24)) in equation (16) alone provides the best fit to the data, thereby indicating that the $T^{5/2}$ term becomes important for $T > 0.7T_C$. (This result is consistent with our earlier (Kaul 1983a) finding.) (ii) Regardless of the temperature range chosen for the fit, inclusion of the $T^{5/2}$ term in addition to the $T^{3/2}$ and T^2 terms does not bring forth any improvement in the quality of the fit; on the contrary, in most cases *reduced* χ^2 assumes larger values and the fit parameters, except for D_0, exhibit erratic variation with t_{max}. (Note that when such an analysis for a number of t_{max} values ranging between 0.4 and 0.95 did not yield encouraging results, this attempt was abandoned. The results of this analysis are not displayed in this work because they are not as exhaustive as those shown in figures 5–7 for the reason mentioned above.) (iii) The variation of spin-wave stiffness coefficient with temperature in the entire temperature range from 0 to $0.95T_C$ is better described by equation (24) than by equation (25). (iv) Considerable deterioration in the quality of theoretical fits occurs and the fit parameters undergo a large but monotonic variation with increasing t_{max} when $\Delta m(H, T)$ data are fitted to the $T^{3/2}$ power law alone, more so in the case where $D(T)$ is set equal to D_0 (figure 5).

Similar fits to the magnetization data taken at different external magnetic field values yield the same results, i.e. values for the fitting parameters D_0, D_2, $D_{5/2}$, β and S are identical to those shown in figures 5–7. The observations (i)–(iv) mentioned above also hold for the alloy a-$Fe_{91}Zr_9$. The final values of the parameters for the alloys in question are: $D_0 = 32 \pm 1$ (29 ± 1) meV Å^2, $D_2 = 1.55 \pm 0.15$ (2.0 ± 0.2) $\times 10^{-6}$ K^{-2}, $D_{5/2} = \beta = 0$ and $S = 1.0 \pm 0.2$ (1.5 ± 0.2) $\times 10^{-6}$ K^{-2} for $T \leq T^*(H)$, where T^* is field-dependent and increases from $\simeq 0.7T_C$ at $H = 5$ kOe to $\simeq 0.85T_C$ at $H = 15$ kOe; and $D_0 = 32 \pm 1$ (29 ± 1) meV Å^2, $D_2 = 1.5 \pm 0.1$ (2.0 ± 0.2) $\times 10^{-6}$ K^{-2}, $D_{5/2} = S = 0$ and $\beta = 0.15 \pm 0.01$ (0.20 ± 0.02) Å^2 for $T^*(H) \leq T \leq 0.95T_C$ in the case of a-$Fe_{90}Zr_{10}$ (a-$Fe_{91}Zr_9$). While the D_0/T_C ratio of 0.137 ± 0.005 (0.138 ± 0.005) meV Å^2 K^{-1} is quite close to that usually found (Kaul and Mohan Babu 1989) in amorphous ferromagnets with competing interactions, the findings that S and D_2 have considerably large values *typical* of Invar systems (Nakai *et al* 1983) and equation (24) describes $D(T)$ better than equation (25) are consistent with our earlier (Kaul 1983a) conclusion that these alloys exhibit weak itinerant ferromagnetism. Moreover, the range of exchange interactions as calculated from the value of $\beta = \langle r^2 \rangle/20$ extracted from the LS fits comes out to be of the order of the nearest-neighbour distance; a finding in consonance with the result that the D/T_C ratio possesses a value the same as that ($(D/T_C) = 0.14$ meV Å^2 K^{-1}) predicted (Kaul 1983b) for a three-dimensional ferromagnet in which direct exchange interactions of Heisenberg form are confined to the nearest neighbours only. A comparison between the spontaneous magnetization and 'in-field' magnetization data demonstrates that the value of D_0 deduced from $M(0, T)$ data is about 75% of that extracted from the $M(H, T)$ data whereas both the sets of data yield nearly the same values (within the error limits) for the quantities D_2 and S. This discrepancy between the values of D_0 should not be taken to imply that the spin-wave stiffness coefficient is field-dependent but instead should be viewed as signalling the softening of spin-wave modes as the re-entrant spin-glass-like behaviour sets in at low temperatures (Hiroyoshi and Fukamichi 1982, Kaul 1983a); a result consistent with the outcome of our Mössbauer measurements (Siruguri *et al* 1988, 1990) on the same sample. However, some element of caution is needed in giving serious consideration to the absolute value of D_0 arrived at by fitting the $M(0, T)$

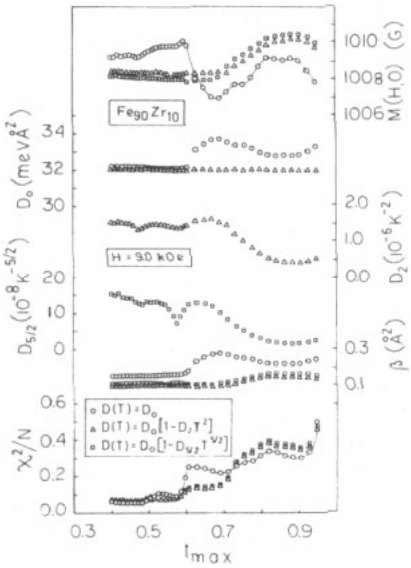

Figure 7. Variation of the free fitting parameters with the upper limit (t_{max}) of the temperature range $t_{min} \leq t = (T/T_C) \leq t_{max}$ when t_{min} is fixed at 0.3 and the least-squares fits to the $M(H = 9\ \text{kOe}, T)$ data are attempted based on equations (16) and (17) with $\Delta m_{vp} = 0$ in equation (16) and $D(T)$ in equation (17) given by either $D(T) = D_0$, open circles, or equation (24), open triangles, or equation (25), open squares.

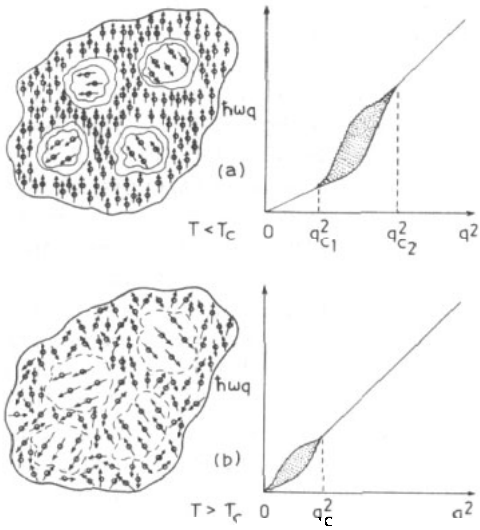

Figure 8. Schematic depiction of the infinite ferromagnetic matrix plus finite spin clusters model for (*a*) $T < T_C$ and (*b*) $T > T_C$ and the spin-wave dispersion relation that it predicts for (*a*) $T < T_C$ and (*b*) $T > T_C$.

data because, in view of the well known observation (Hiroyoshi *et al* 1983, Krishnan *et al* 1984, Ryan *et al* 1987) that the magnetization in these alloys does not saturate even in fields as intense as 190 kOe at low temperatures, an extrapolation to zero field may not yield reliable values for $M(0, T)$ at temperatures below the re-entrant transition temperature when the highest field used in this work is merely 15 kOe. The values for various parameters, including D_0, deduced from the 'in-field' magnetization data should, therefore, be regarded as more reliable.

3.3. A phenomenological model

In view of the *field-independent* value of the spin-wave stiffness coefficient D_0 deduced from the present measurements, the dependence of D_0 on H reported (Krishnan *et al* 1984, Beck and Kronmüller 1985) earlier could be an artifact of the analysis, which attributes the observed thermal demagnetization to either spin-wave or single-particle contribution alone. But the disagreement between the results of bulk magnetization measurements, which strongly indicate the existence of well-defined spin-wave excitations, and inelastic neutron scattering experiments (Fish and Rhyne 1987), which do not show any evidence for discrete propagating spin waves for $T < T_C$ within the energy resolution limit of 120 μeV, is apparently hard to reconcile. In order to resolve this *apparent contradiction*, recourse is taken to the three-dimensional (3D) ferromagnetic

(FM) matrix plus finite spin clusters picture (Kaul 1984a, 1985). Though a brief account of this model can be found elsewhere (Kaul 1984a, 1985, 1988, Kaul *et al* 1988), more details about the same are given in this paper. In this model, it is postulated that (*a*) the spin system for $T < T_C$ consists of an *infinite* 3D FM matrix and *finite* spin clusters (composed of a set of ferromagnetically coupled spins), which are embedded in, but 'isolated' from, the FM matrix by zones of frustrated spins surrounding the finite clusters, (*b*) a wide distribution in the size of spin clusters exists, and (*c*) the isolation between the spin clusters and the FM matrix is not complete, i.e. the long-range RKKY interactions provide a *weak* coupling between the clusters and the FM matrix and also between the clusters themselves. The mechanism that could lead to such a spin structure is elucidated below. By virtue of the fact that in the melt quenching process the cooling rate is not uniform throughout the melt, the nearest-neighbour (NN) distance between the atoms varies erratically from one portion of the non-crystalline solid to the other, so much so that the *average* NN distance is appreciably greater in certain *microscopic* regions than in the remaining bulk. Considerable mismatch in the NN interatomic spacings is, therefore, expected to occur within the zones that separate these microscopic regions from the bulk. As a consequence of this mismatch, large 'quenched-in' *local* stresses exist in these zones. For a magnetic alloy system in which the majority of the atoms bear a magnetic moment, the microscopic regions and the bulk can be identified as the finite spin clusters and infinite matrix, respectively. If the average NN distance between the spins (moments) in the matrix just exceeds the critical distance r_c at which the exchange integral changes sign in the Bethe–Slater curve, ferromagnetic coupling exists not only between the spins constituting the matrix but also between those forming the clusters (ferromagnetic coupling being stronger in the latter case than in the former); whereas the spins contained in the zones surrounding the clusters get 'frustrated' due to both a sizable magnetostrictive coupling (particularly in the Invar systems like the amorphous alloys in question) between the spins and the 'lattice' and *competing* interactions between the spins originating from the fluctuation in the value of the NN interatomic spacing (or the spacing between the NN spins) around r_c within these zones. Having provided a logical basis for the 3D FM matrix plus finite spin clusters picture (figure 8(*a*)), an explanation for the absence of spin-wave-like features in the inelastic neutron scattering (INS) spectra taken in a certain wavevector transfer range is now attempted in terms of this model. Though spin waves, whose stiffness is controlled by the strength of exchange interaction between spins in the FM matrix, are excited for all wavevectors in the infinite ferromagnetic matrix at temperatures $T < T_C$, all of them do not propagate through the matrix unhindered for the following reason. The spin waves for which q falls within the range $q_{c1} \lesssim q \lesssim q_{c2}$, where q_{c1} and q_{c2} are the caliper dimensions of the smallest (largest) and the largest (smallest) spin cluster in the wavevector (direct) space, get *severely damped* due to coupling to, and intense scattering from, the finite spin clusters. Thus, if the INS measurements are performed in the wavevector range $q_{c1} \lesssim q \lesssim q_{c2}$, only a broad 'diffusive-like' spectrum with no propagating features would be observed at any temperature below T_C. By contrast, constant-q scans recorded at the wave-vector values that lie outside this q range should exhibit well-defined spin-wave peaks for all temperatures below T_C but the nature and origin of these spin waves now depend on whether $q < q_{c1}$ or $q > q_{c2}$. In the long-wavelength limit (i.e. when $q < q_{c1}$), well-defined spin waves can be excited in the FM matrix only and that too at temperatures well below T_C because of the low energy cost involved, and such spin waves propagate through the matrix without any significant damping. On the contrary, in the short-wavelength limit (i.e. when $q > q_{c2}$) spin waves can be excited in the FM matrix as well as in the finite

clusters either at very high incident neutron energies when the temperature is low or at high temperatures for the range of incident neutron energies conventionally used, but in this case the FM spin waves are expected to get damped due to strong exchange fluctuations (caused by the fluctuation in the NN distance between spins) as contrasted with the intra-cluster spin waves, which should be relatively well defined because the exchange coupling between the spins within the clusters is much stronger and has a much narrower distribution. Thus, the INS spectra should consist of reasonably sharp spin-wave peaks signalling the existence of intra-cluster spin-wave excitations superimposed on very broad 'diffusive-like' structure arising from the overdamped FM spin waves. The magnon dispersion relation for all q and $T < T_C$ is schematically depicted in figure 8(a). Note that the slope of $\hbar\omega_q$ versus q^2 straight line, i.e. the spin-wave stiffness coefficient, is larger for $q \gtrsim q_{c2}$ than for $q \lesssim q_{c1}$ because the exchange coupling between the spins in the clusters is much stronger compared to that in the FM matrix. As the temperature is increased through T_C, exchange coupling between spins in the FM matrix weakens, the frustration zones start 'melting' away and the finite clusters grow in size by polarizing spins (some of the spins) originally belonging to the frustration zones (the FM matrix) and interact with one another through individual spins of the matrix. For $T > T_C$, the long-wavelength spin waves characteristic of the FM matrix are completely absent and well-defined intra-cluster spin waves can be excited only for $q \gtrsim q_c$ (figure 8(b)) but now $q_c \ll q_{c2}$. Considering our earlier finding (Kaul 1988) that in these amorphous alloys the *average* size of the finite spin clusters for $T \lesssim T_C$ is $\simeq 25$ Å, the range of q values ($0.05\,\text{Å}^{-1} \leqslant q \leqslant 0.12\,\text{Å}^{-1}$) covered in the inelastic neutron scattering measurements (Fish and Rhyne 1987) falls well within the range $q_{c1} \leqslant q \leqslant q_{c2}$ in figure 8(a) where the spin-wave excitations in the FM matrix are strongly damped and hence no resolvable spin-wave peaks are found in the INS spectra. In view of the foregoing arguments, the INS measurements for $T < T_C$ need to be extended to q values *low enough* ($q \ll 0.05\,\text{Å}^{-1}$) to observe well-defined spin waves, characteristic of the 3D FM matrix (bulk), whose stiffness has been determined in this work.

Other important physical implications of this model are as follows. According to this model, weak itinerant-electron ferromagnetism and Invar behaviour are *inherent* properties of the FM matrix whereas the thermomagnetic and thermoremanent effects (Hiroyoshi and Fukamichi 1982, Kaul 1983a), asymmetric hysteresis loops (Hiroyoshi and Fukamichi 1982) and a rapid increase in the small-angle neutron scattering response (Rhyne and Fish 1985, Rhyne *et al* 1988) as well as in the *average* hyperfine field (Ghafari *et al* 1988, Siruguri *et al* 1988, 1990) at low temperatures are *characteristic* properties of the 'mixed magnetic state', which comes into existence when the weakly interacting finite spin clusters *freeze* in random orientations and *coexist* with the FM matrix at a temperature T_f as the sample temperature is lowered towards 0 K. In the mixed state, large *local* random anisotropy fields develop at the interface between the frozen clusters and the FM matrix and the coercivity increases steeply (Beck and Kronmüller 1985, Ryan *et al* 1987) as a result of the pinning of domain walls by the *frozen ferromagnetic* clusters embedded in the FM matrix. The irreversibility of the low-field magnetization at low temperatures and precipitous decline in the 'zero-field-cooled' magnetization for $T < T_f$ can be satisfactorily explained by properly correcting for the self-demagnetization effects (Beck and Kronmüller 1985, Read *et al* 1986) brought about by the presence of the exponentially increasing coercivity and the concomitant magnetic hardness (magnetic anisotropy energy). Another interesting consequence of large *local* random anisotropy fields in the mixed state is that they randomize spins in the immediate vicinity of the cluster boundaries, and these randomized spins, in turn, give rise to *slight canting* of the

spins in the FM matrix. The canted spin arrangement not only results in a reduction of the net exchange coupling between spins and thereby leads to the softening of the FM spin waves (an inference in agreement with our observation) but also makes the saturation in magnetization extremely hard to achieve (a deduction consistent with the experimental observations of Hiroyoshi *et al* (1983), Krishnan *et al* (1984) and Ryan *et al* (1987)).

4. Conclusions

High-precision magnetization data taken on amorphous $Fe_{90}Zr_{10}$ and $Fe_{91}Zr_9$ alloys at temperatures ranging from 4.2 to 300 K in external magnetic fields up to 15 kOe permit us to draw the following conclusions.

The temperature dependence of the spontaneous magnetization in the investigated temperature range is adequately described by a theory that goes beyond the conventional Stoner model in including both transverse and longitudinal fluctuations in the local spin density.

For temperatures well outside the critical region, $M(H, T)$ data at high fields satisfy the magnetic equation of state predicted by the modified Stoner model.

While both spin-wave and Stoner single-particle excitations contribute to thermal demagnetization at low temperatures, enhanced fluctuations in the local magnetization give a dominant contribution over a wide range of intermediate temperatures and for temperatures close to the Curie temperature when the external magnetic field is absent.

Spin fluctuations get strongly suppressed by the external magnetic field.

The spin-wave stiffness coefficient D is *independent* of the external field and D/T_C ratio possesses a value of $\simeq 0.14$ typical of amorphous ferromagnets with competing interactions.

Softening of spin-wave modes takes place at low temperatures.

Competing interactions confine the direct Heisenberg exchange interaction to the nearest neighbours only.

A model, originally proposed by the author to explain critical phenomena in amorphous ferromagnetic alloys, is shown to provide a straightforward explanation not only for the absence of spin-wave peaks in the inelastic neutron scattering spectra taken in the wavevector transfer range of $0.05\ \text{Å}^{-1} \leq q \leq 0.12\ \text{Å}^{-1}$, but also for other diverse aspects of magnetism in the glassy alloys in question.

Acknowledgments

The author thanks Mr P D Babu for his help in the computations and the referees for their useful suggestions.

References

Beck W and Kronmüller H 1985 *Phys. Status Solidi* b **132** 449
Edwards D M and Wohlfarth E P 1968 *Proc. R. Soc.* A **303** 127
Fish G E and Rhyne J J 1987 *J. Appl. Phys.* **61** 454
Ghafari M, Keune W, Brand R A, Day R K and Dunlop J B 1988 *Mater. Sci. Eng.* **99** 65
Hiroyoshi H and Fukamichi K 1982 *J. Appl. Phys.* **53** 2226

Hiroyoshi H, Fukamichi K, Hoshi A and Nakagawa Y 1983 *High Field Magnetism* ed M Date (Amsterdam: North-Holland) p 113
Izuyama T and Kubo R 1964 *J. Appl. Phys.* **35** 1074
Kaul S N 1983a *Phys. Rev.* B **27** 6923
—— 1983b *Phys. Rev.* B **27** 5761
—— 1984a *IEEE Trans. Magn.* **MAG-20** 1290
—— 1984b *Solid State Commun.* **52** 1015
—— 1985 *J. Magn. Magn. Mater.* **53** 5
—— 1987 *J. Appl. Phys.* **61** 451
—— 1988 *J. Phys. F: Met. Phys.* **18** 2089
Kaul S N, Bansal C, Kumaran T and Havalgi M 1988 *Phys. Rev.* B **38** 9248
Kaul S N, Hofmann A and Kronmüller H 1986 *J. Phys. F: Met. Phys.* **16** 365
Kaul S N and Mohan Babu T V S M 1989 *J Phys.: Condens. Matter* **1** 8509
Kaul S N and Siruguri V 1991 *J. Phys.: Condens. Matter* submitted
Kaul S N and Veera Mohan Ch 1991 *J. Phys.: Condens. Matter* **3** 2703
Kaul S N, Veera Mohan Ch, Babu P D, Sambasiva Rao M and Lucinski T 1990 unpublished
Keffer F 1966 *Encyclopedia of Physics* vol XVIII, ed H P J Wijn (Berlin: Springer) part 2, p 1
Krishnan R, Rao K V and Liebermann H H 1984 *J. Appl. Phys.* **55** 1823
Lonzarich G G and Taillefer L 1985 *J. Phys. C: Solid State Phys.* **18** 4339
Mathon J and Wohlfarth E P 1968 *Proc. R. Soc.* A **302** 409
Moriya T 1979 *J. Magn. Magn. Mater.* **14** 1
—— 1983 *J. Magn. Magn. Mater.* **31–34** 10
Moriya T and Kawabata A 1973 *J. Phys. Soc. Japan* **34** 639; **35** 669
Nakai I, Ono F and Yamada O 1983 *J. Phys. Soc. Japan* **52** 1791
Obi Y, Wang L C, Motsay R, Onn D G and Nose M 1982 *J. Appl. Phys.* **53** 2304
Read R A, Moyo T and Hallam G C 1986 *J. Magn. Magn. Mater.* **54–57** 309
Rhyne J J, Erwin R W, Fernandez-Baca J A and Fish G E 1988 *J. Appl. Phys.* **63** 4080
Rhyne J J and Fish G E 1985 *J. Appl. Phys.* **57** 3407
Ryan D H, Coey J M D, Batalla E, Altounian Z and Ström-Olsen J O 1987 *Phys. Rev.* B **35** 8630
Shirakawa K, Ohnuma S, Nose M and Masumoto T 1980 *IEEE Trans. Magn.* **MAG-16** 910
Siruguri V, Kaul S N, Rajaram G and Chandra G 1988 *Proc. Solid State Phys. Symp. India* **31C** 233
—— 1990 *Annales Fis.* B **86** 181
Takeuchi J and Masuda Y 1979 *J. Phys. Soc. Japan* **46** 468